

A Predictive Factor For Short-Term Outcome In Patients With COVID-19: CT Score For Lung Involvement

Wang G¹, Ma K², Yu N³, Liu F³, Luan Z², Zhao C⁴, Wang J¹, Qin Z³, Li W⁵, Liu B⁶, Liu Y⁷, Niu M¹, Xiao W⁸, Wang Z^{9*}

¹Department of Radiology, The First Affiliated Hospital of China Medical University, China

²Department of critical care medicine, The First Affiliated Hospital of China Medical University, China

³Department of pulmonary and critical care medicine, The First Affiliated Hospital of China Medical University, China

⁴Department of Otolaryngology, the First Affiliated Hospital of China Medical University, China

⁵Department of thoracic surgery, The First Affiliated Hospital of China Medical University, China

⁶Department of Cardiac Surgery, The First Affiliated Hospital of China Medical University, China

⁷Department of ultrasonography, The First Affiliated Hospital of China Medical University, China

⁸Department of Anesthesiology, Union Hospital, Tongji Medical College, Huazhong University of Science, China

⁹Department of Surgical Oncology, The First Affiliated Hospital, China Medical University, Shenyang, China

*Corresponding author:

Zhenning Wang,

Department of Surgical Oncology, The First Affiliated Hospital of China Medical University, 155 Nanjing North Street, Shenyang 110001, China, E-mail: josieon826@sina.cn

Received: 02 Mar 2021

Accepted: 24 Mar 2021

Published: 30 Mar 2021

Copyright:

©2021 Wang Z. This is an open access article distributed under the terms of the Creative Commons Attribution License, which permits unrestricted use, distribution, and build upon your work non-commercially.

Keywords:

COVID-19; SARS-CoV-2; CT score for lung involvement

Abbreviations

95%CI = 95% confidence interval, ARDS = Acute Respiratory Distress Syndrome, COVID-19 = coronavirus disease, GGO = Ground-Glass Opacity, ICC = Intraclass Correlation Coefficient, MERS = Middle East Respiratory Syndrome, OR = Odds Ratio, SARS-CoV-2 = Severe Acute Respiratory Syndrome Coronavirus 2, SpO₂ = Peripheral Capillary Oxygen Saturation.

1. Abstract

1.1. Background: Recently, typical CT features of coronavirus disease (COVID-19) pneumonia have been reported. However, the prognostic value of CT evaluations has not been fully elucidated.

1.2. Methods: In this retrospective, multi-center cohort study, we reviewed 645 patients who had died or recovered from laboratory-confirmed COVID-19 between January 23, 2020 and March 6, 2020 in two hospitals in Wuhan and Shenyang, China. Demographic, clinical, laboratory, and CT data were extracted and compared between the non-survivor and survivor group. Multivariable logistic regression analysis identified risk factors for in-hospital death.

1.3. Results: This study enrolled 253 patients (63 died in the hospital, 190 were discharged). Compared to survivors, non-survivors were older, mostly male, had a higher prevalence of preexisting comorbidity, higher incidences of hypoxemia, lymphopenia and bacterial coinfection ($p < 0.001$ for each). Regarding CT evaluations, non-survivors had higher CT scores (14.3 ± 3.4 vs. 8.1 ± 2.9), higher incidences of bronchial dilation with mosaic (34.9% vs. 10.5%), emphysema (28.6% vs. 10.5%), and diffuse opacity distribution (76.1% vs. 36.8% ; all $p < 0.001$). Multivariable regression analysis showed that increasing odds of in-hospital death were associated with preexisting comorbidity (OR=12.48, 95% CI: 1.48–105.07; $p=0.020$), lower peripheral capillary oxygen saturation (per 1% increase OR=0.681, 95%CI: 0.50–0.93; $p=0.016$), bacterial coin-

Citation:

Wang Z, A Predictive Factor For Short-Term Outcome In Patients With COVID-19: CT Score For Lung Involvement. *Ame J Surg Clin Case Rep.* 2021; 2(7): 1-8.

Authors contributed:

Wang G, Ma K and these authors are contributed equally to this work.

fection (OR=10.73, 95%CI: 1.01–114.01; $p=0.049$), and higher CT involvement scores (per 0.5-point increase OR=1.41, 95%CI: 1.04–1.91; $p=0.028$).

1.4. Conclusion: The CT involvement score is a potential predictor of short-term outcomes in patients with COVID-19. A thorough assessment combining CT evaluation with demographic and clinical information may help establish risk stratifications and optimize treatment decisions at an early stage.

2. Introduction

The coronavirus disease 2019 (COVID-19) is caused by severe acute respiratory syndrome coronavirus 2 (SARS-CoV-2, previously known as 2019-nCoV). First reported in Wuhan, China on December 31, 2019, it has become the most serious public health crisis of our generation and has a profound impact on the global economy and geopolitics (1–4). By March 2021, SARS-CoV-2 has infected more than 1.17 billion individuals and resulted in about 2.58 million deaths in 235 countries, areas or territories worldwide [5].

COVID-19 pneumonia is the most common clinical presentation of patients infected with SARS-CoV-2. Chest CT is considered the first-line imaging modality in highly suspected cases and reportedly more sensitive than real-time reverse transcription-polymerase chain reaction tests in the early verification of suspected COVID-19 cases [6–9]. Recently published radiographic studies have advanced our knowledge of this novel viral pneumonia, most of them focusing on its CT features. Most of these typical features are similar to those of other viral infections of the lung such as SARS and Middle East respiratory syndrome (MERS) [10,11]. However, the more prominent CT image characteristic is the extent of the lung involvement that, besides the early detection of a pulmonary infection, may provide information regarding the prognosis of COVID-19 patients.

Several studies recently published in *Lancet* [1,12–13] revealed that the mortality of COVID-19 is related to Acute Respiratory Distress Syndrome (ARDS), and postmortem biopsies showed evident desquamation of pneumocytes and hyaline membrane formation in a patient who had died from severe infection with SARS-CoV-2 [14]. Previous studies demonstrated that CT evaluation is feasible to predict the prognosis of ARDS [15–18]. Furthermore, Chen et al reported that the characteristics of patients who had died from COVID-19 were in line with the MuLBSTA score [2], an early warning model for predicting mortality in viral pneumonia. In this scoring system, the predominant index is the multi-lobular infiltration [19].

According to recent reports, bilateral multiple infiltrates are also common CT manifestations in COVID-19 patients, especially in those with life-threatening pneumonia [13]. The extent of lung involvement can be evaluated from chest CT images.

This study aims to investigate whether CT-evaluated lung in-

volvement is of predictive value for the prognosis in patients with COVID-19 pneumonia.

3. Materials and Methods

3.1. Study Design and Patients

The current study was approved by the Ethics of Committees of The First Affiliated Hospital of China Medical University and the Union Hospital, Tongji Medical College, Huazhong University of Science and Technology. The requirement for informed consent was waived for this retrospective study since anonymous data were analyzed. This retrospective study included two adult patient (≥ 18 years old) cohorts in the Union Hospital and The First Affiliated Hospital of China Medical University. We reviewed medical records between January 23, 2020, and March 6, 2020, of SARS-CoV-2-positive patients confirmed by real-time reverse transcription-polymerase chain reaction and identified 645 consecutive patients who had died or been discharged in this period. After excluding 392 patients without available key information such as sequential CT scans during the progress of the pulmonary infiltrate, 253 patients were finally included of whom 63 patients died during hospitalization and 190 were discharged. The number of days between symptom onset and date of outcome was tracked.

3.2. Demographic, Clinical, and Laboratory Data

Data for demographic, clinical, and laboratory parameters including age, sex, preexisting comorbidities, treatment modality, peripheral capillary oxygen saturation (SpO₂) on admission, bacterial coinfection, and routine laboratory examinations were collected for analysis.

3.3. CT Imaging and Evaluation

Chest CT scans without intravenous contrast were performed with the patient in the supine position during end-inspiration using one of three multi-detector CT scanners (Ingenuity Core128, Philips Medical Systems, Netherlands; SOMATOM Definition AS, Siemens Healthineers, Germany; Discovery CT750 HD, GE Healthcare, US). For CT acquisition, the tube voltage was 120 kVp with automatic tube current modulation. Using standard algorithms, CT images were reconstructed with a slice thickness of 0.625 mm or 1.5 mm and a reconstruction interval of 0.625 mm or 1.5 mm, respectively, as 512×512 axial images.

On average, each patient enrolled underwent 2.7 ± 0.7 longitudinal CT scans. All CT images were scored independently by two radiologists blinded to the clinical characteristics with more than 12 years of experience in thoracic radiology. The descriptions of thin-section CT findings were based on the recommendations of the Nomenclature Committee of the Fleischner Society [20] and previous studies [21–23]. Predominant CT manifestations were categorized as Ground-Glass Opacification (GGO), consolidation, reticulation (coarse linear or curvilinear opacities, fine subpleural reticulations), mixed pattern (a combination of consolidation, GGOs, and reticular opacities in the presence of architectural

distortion), honeycombing, and crazy-paving (smooth interlobular septal thickening superimposed on GGOs). The presence of bronchial dilation associated with any of these findings and underlying CT abnormalities such as emphysema were also noted. Pneumothorax, pneumo mediastinum, and pleural effusion were also recorded.

CT images of the day with the maximum infiltrate extent, termed hereafter “peak stage”, were selected to evaluate lung involvement, and the number of days from initial symptom onset to the time of this CT acquisition was considered as the peak stage time of the lung involvement. All evaluations were conducted in a lung window (level: -600 HU, width: 1,500 HU). The bilateral lungs were divided into 20 segments based on symmetric anatomy (the apicoposterior segment of the left upper lobe and the anteromedial segment of the left lower lobe were both considered as two segments). Each segment involvement was semi-quantitatively scored from 0 to 1 according to the involved area: 0 point, no involvement; 0.5 points, $\leq 50\%$ involvement; 1 point, $>50\%$ involvement. The total CT score was the sum of all individual segment scores and ranged from 0 to 20 points (24). Additionally, the distribution pattern of the opacities was classified into three categories: 1) sub-pleural, 2) multifocal, or 3) diffuse. A case illustration for this CT scoring procedure is provided in (Figure 1).

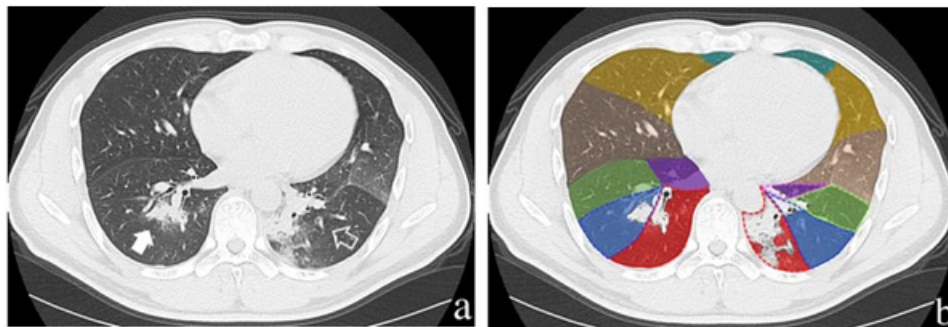


Figure 1: Illustration of CT scores evaluating the lung involvement in a CT image with bilateral infiltration of the lower lobes. A traverse Chest CT image acquired on day 10 after symptom onset displaying consolidation of the right (a, closed arrow) and left (a, open arrow) lower lobes in a 41-year-old male patient with COVID-19. (b) Schematic diagram showing that the opacity of the right lower lobe was located in the lateral (blue) and posterior (red) segments, while the opacity of the left lower lobe was located in the medial (purple), anterior (green), lateral (blue), and posterior (red) segments. CT scoring: For the posterior segment of the right lower lobe, the involvement extent was scored 1 point, because the involved area was greater than 50% of the corresponding segment area. For the other five involved segments, the involvement extent was scored 0.5 points for each, because the involved areas were smaller than 50% of their respective segment areas.

3.5. Results

Age, preexisting comorbidity and lymphocyte count were included because previous studies indicate that they are factors related to the mortality risk in COVID-19 pneumonia [1,25,26]. Since some asymptomatic underlying pulmonary diseases such as emphysema impair the restoration of pulmonary functions, they were also analyzed in lung CT images as underlying abnormalities.

3.6. Patient Characteristics and Clinical Parameters

The median age of the finally included 253 patients was 61.0 years (IQR 49.5–69.0, range 21–88), and 132 (52.1%) patients

3.4. Statistical Analyses

All statistical analyses were performed using SPSS (IBM Statistics 24, New York, US). Continuous normally distributed data are expressed as the mean \pm SD, non-normal data as median with IQR. Continuous variables were compared using the paired Student’s t-test or Mann-Whitney U test, whereas the χ^2 or Fisher’s exact tests were used for categorical dependent variables, as appropriate. Two-way mixed consistency Intraclass Correlation Coefficients (ICCs) were analyzed to evaluate inter- and intra-observer agreements. p-values <0.05 were considered statistically significant.

A binary logistic regression model was used to investigate possible factors that might influence the prognosis. Seven variables were included in this regression model: the five categorical variables, namely, male sex, comorbidity, predominant CT manifestation, opacity distribution, and underlying CT abnormality and the four continuous variables, namely, CT score, age, SpO₂, and lymphocyte count. Categorical variables were dichotomized and assigned values as follows: male sex (female=0, male=1), comorbidity (absence=0, presence=1), and bacterial coinfection (absence=0, presence=1). For all categorical analyses, “0” was set as the reference. The outcome of patients with COVID-19 was set as the dichotomous dependent variable (discharge from hospital=0, death=1).

were male. Compared to the survivor group (n=190), the non-survivor group (n=63) comprised older (p<0.0001) and more male (p<0.001) patients. The median time from illness onset to discharge was 18.5 \pm 5.7 days, whereas the median time to death was 9.0 \pm 8.3 days (p<0.0001).

A total of 100 (39.5%) patients had comorbidities, with hypertension being the most commonly observed in 44 (17.4%) patients, followed by diabetes, coronary heart diseases, malignancies, gastrointestinal diseases, chronic obstructive pulmonary disease, renal disease, stroke, and liver diseases. During hospitalization,

26 (10.2%) patients presented a bacterial coinfection. Lymphopenia and hypoxemia occurred in 63 (24.9%) and 71 (28.1%) of the patients, respectively. Compared to survivors, non-survivors had higher incidences of comorbidity, hypoxemia, lymphopenia, and bacterial coinfection. Additional details are provided in (Table 1).

4. CT Findings

CT images at peak stage were selected to be reviewed and scored. The median time from illness onset to this CT scan was 10.0 days (range 7.0–14.0). Sequential CT images of a patient from the survivor group show the development of lung infiltrates (Figure 2).

Table 1: Demographics and Clinical Characteristics

Parameters	All patients (n=253)	Non-survivor group (n=63)	Survivor group (n=190)	p-value
Age (y)	61 (49.5, 69.0)	69 (58.5, 78.0)	58 (47.3, 58.0)	0.0001
Range	21–88	21–88	23–85	
Sex (Male)	132 (52.1)	44 (69.8)	88 (46.3)	0.001
Comorbidity	100 (39.5)	48 (76.2)	52 (27.3)	0.0001
Hypertension	44 (17.4)	24 (38.1)	20 (10.5)	
Diabetes	21 (8.3)	9 (14.3)	12 (6.3)	
Coronary heart disease	20 (16.2)	8 (12.7)	12 (6.3)	
Malignancy	19 (7.5)	13 (20.6)	6 (3.2)	
Gastrointestinal disease	17 (6.7)	5 (7.9)	12 (6.3)	
COPD	16 (6.3)	6 (9.5)	10 (5.3)	
Renal disease	10 (3.9)	6 (9.5)	4 (2.1)	
Stroke	6 (2.3)	4 (6.3)	2 (1.1)	
Liver disease	4 (1.6)	2 (3.2)	2 (1.1)	
Clinical				
SpO2	91.8±8.8	81.6±12.6	95.1±2.8	0.0001
Lymphocyte count	1.0±0.6	0.5±0.3	1.2±0.5	0.0001
Coinfection	26 (10.2)	18 (28.5)	8 (4.2)	0.0001
Length of hospital stay	16.0±7.9	9.0±8.3	18.5±5.7	0.0001

Continuous parameters were presented as the mean±SD and compared using paired Student’s t-test or Mann-Whitney U test, categorical data were presented as n (%) and compared using χ^2 or Fisher’s exact tests. p-values represent the comparison between non-survivor and survivor groups. COPD = chronic obstructive pulmonary disease, SpO2 = peripheral capillary oxygen saturation. SD= standard deviation.

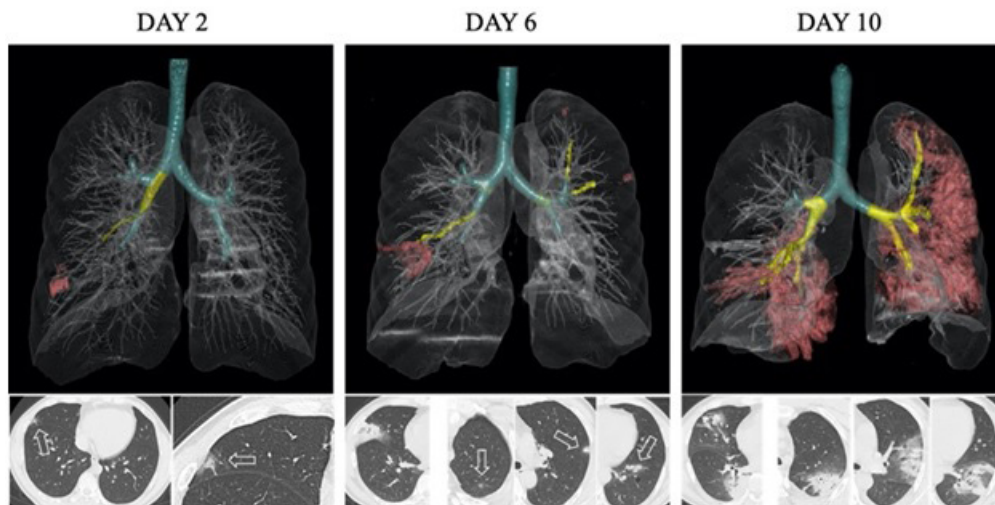


Figure 2: Progressively developing lung infiltrates on sequential CT images of a 37-year-old male patient with COVID-19. Chest CT images acquired 2 days after symptom onset show focal ground-glass opacities combined with consolidation in the lateral segment of the right middle lobe. The following CT acquired on day 6 after symptom onset reveals three new subpleural opacities in the left lung, and the lung infiltrates show maximal bilateral involvement on day 10 after onset. Sequential 3D volume-rendered images demonstrate the pulmonary involvement developing over time.

4.1. The CT findings of the study population were summarized by category as follows:

Predominant CT manifestation The mixed pattern was found in 146 (57.7%) of the 253 patients, consolidation in 29 (11.5%), reticulation in 18 (7.1%), GGO in 33 (13.0%), crazy-paving in 18 (7.1%), and honeycombing in 9 (3.6%).

The compositions of predominant CT manifestations were compa-

parable between the two study groups (p=0.231). The mixed pattern consisting of GGO, consolidation, and reticulation was the predominant CT manifestation in both groups.

Bronchial dilation Bronchial dilations were found in 167 (66.0%) patients. The dilations in 157 (62.1%) of those were surrounded by one or more CT features including reticulation, consolidation, or honeycombing. Besides, 42 (16.6%) presented with mosaic atten-

uation in the lung parenchyma (Figure 3 and Figure 4).

The incidences of bronchial dilations detected with CT were similarly high in both non-survivor and survivor groups ($p=0.644$). Bronchial dilation surrounded by reticulation, consolidation, or honeycombing was suggestive of traction bronchiectasis, and there was no significant difference in detection frequency between the two groups ($p=0.977$). However, the frequency of bronchial dilation presenting with mosaic attenuation was significantly higher in the non-survivor group than in the survivor group ($p<0.001$). Underlying CT abnormalities Emphysemas were found in 38 (15.0%) of the 253 enrolled patients. The incidence of emphysemas presenting in the non-survivor group was higher than that in the survivor group (Table 2).

Distribution Three lung infiltrate distribution patterns were identified, as mentioned in the method section. Among all 253 patients, opacities presented a diffuse pattern in 118 (46.6%) cases, a subpleural pattern in 93 (36.8%), and a multifocal pattern in 42 (16.6%). Infiltrates presented in both non-survivor and survivor groups with a lower lobe predilection.

These distributions of lung infiltrates were significantly different between the two groups ($p<0.0001$). Infiltrates on CT images of non-survivors were more likely to present with bilateral diffuse opacity in both peribronchial and subpleural areas (Table 2).

CT score Both inter reviewer and intra reviewer agreements were excellent with ICCs of 0.966 (95%CI 0.936–0.994) and 0.952 (95%CI 0.934–0.989), respectively. The final score for each lung segment was calculated as the mean of the two reviewers' scores. The mean CT score for the total of 253 patients was 9.8 ± 4.2 points, and the lower lungs contained segments with the highest involvement score (2.7 ± 1.2), followed by the middle (1.8 ± 1.4) and upper (1.1 ± 0.8) lungs. The highest score in the lower lobe also confirmed the lower lobe predilection of the infiltrates mentioned above.

The CT scores evaluating the lung involvement extent were higher in the non-survivor group than in the survivor group, both at the whole-lung level and the level of individual lobes (all $p<0.0001$). Indirectly, this result corroborates that most non-survivors presented a diffuse distribution pattern. Additional details are provided in (Table 2).



Figure 3: Bronchial dilation associated with various CT features at the peak stage of the pulmonary infiltrate in patients with COVID-19 pneumonia, Part I. (a) Mosaic hypoattenuation associated with bronchial dilation (arrows) suggestive of air trapping. (b) Crazy-paving associated with bronchial dilation (arrow). (c) Consolidation with bronchial dilation (arrow).

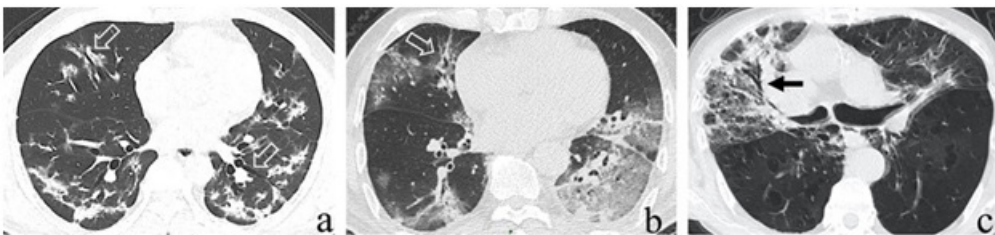


Figure 4: Bronchial dilation associated with various CT features at the peak stage of the pulmonary infiltrate in patients with COVID-19 pneumonia, Part II. (a) Combination of consolidation and reticulation associated with bronchial dilation (arrows). Fine interlobular lines are also visible (black arrow). (b) Reticulation associated with bronchial dilation (arrow). (c) Honeycombing associated with bronchial dilation (arrow).

Table 2: Comparison of Chest CT Findings and CT Scores between the Non-survivors and Survivors with COVID-19

Parameters	Non-survivor group (n=63)	Survivor group (n=190)	p-value
Predominance			0.231
<i>GGO</i>	5 (7.9)	28 (14.7)	
<i>Crazy-paving</i>	2 (3.1)	16 (8.4)	
<i>Consolidation</i>	8 (12.7)	21 (11.1)	
<i>Reticulation</i>	6 (9.5)	12 (6.3)	
<i>Honeycombing</i>	5 (7.9)	4 (2.1)	
<i>Mixed pattern</i>	37 (58.8)	109 (57.4)	
Bronchial dilation	43 (68.3)	124 (65.2)	0.664
<i>Mosaic with bronchial dilation</i>	22 (34.9)	20 (10.5)	0.0001
<i>Traction bronchiectasis</i>	39 (61.9)	118 (62.1)	0.977

Underlying abnormality (emphysema)	18 (28.6)	20 (10.5)	0.001
Distribution			0.0001
<i>Subpleural</i>	5 (7.9)	88 (46.3)	
<i>Multifocal</i>	10 (15.8)	32 (16.8)	
<i>Diffuse</i>	48 (76.1)	70 (36.8)	
CT Score	14.7±3.4	8.1±2.9	0.0001
<i>Right upper lobe</i>	2.1±0.8	1.2±0.7	0.0001
<i>Right middle lobe</i>	1.4±0.5	0.6±0.5	0.0001
<i>Right lower lobe</i>	4.0±1.0	2.4±0.9	0.0001
<i>Left upper lobe</i>	1.6±0.6	0.8±0.6	0.0001
<i>Left lower lobe</i>	3.9±1.2	2.3±1.0	0.0001

Categorical data are presented as numbers of patients (percentages) and compared using χ^2 or Fisher's exact tests. CT scores are present as the mean±SD and compared using paired Student's t-test, the median time from illness onset to this CT scan is 10.0 days (range 7.0–14.0). GGO = ground-glass opacity. SD= standard deviation.

4.2. Correlations between Clinical Parameters, CT Scores, and Outcome:

We included 253 patients with complete data for all variables in the multivariable logistic regression model. We found that pre-existing comorbidities, lower SpO2 values, and higher CT scores were associated with increased odds of death (Table 3).

Specifically, increased CT scores (OR=1.407 per 0.5-point increase, p=0.028), preexisting comorbidity (OR=12.482, p=0.02), and presence of bacterial coinfection (OR=10.731, p=0.049) were risk factors that contributed to the death. By contrast, SpO2 (OR=0.681 per 1% increase in SpO2, p=0.016) was a protective factor. Additional details are provided in (Table 3).

Table 3: Factors Contributing to the Short-time Outcome of Patients with COVID-19

Factors	OR	95%CI	p-value
Age (y)	0.986	0.928–1.047	0.642
Sex (Male)	1.401	0.204–9.611	0.731
Comorbidity	12.482	1.483–105.066	0.02
SpO2	0.681	0.498–0.932	0.016
Lymphocyte count	0.206	0.015–2.794	0.235
Coinfection	10.731	1.010–114.007	0.049
CT involvement score	1.407	1.037–1.911	0.028

Categorical variables: Male sex (female=0, male=1); Comorbidity (absence=0, presence=1); Coinfection (absence=0, presence=1); Underlying lung CT abnormality (absence=0, presence=1); Reference category=0. Continuous variables: Age (years), SpO2 (%), Lymphocyte count (10⁹/L), Length of hospital stay (days), CT involvement score (0–20 points).

95%CI = 95% confidence interval, OR = odds ratio, SpO2 = peripheral capillary saturation of oxygen.

5. Discussion

Risk factors for mortality in patients with COVID-19 have not been fully investigated yet. Compared to survivors, our results identify non-survivors as older, with a higher percentage of males, with higher prevalence of comorbidity, higher incidences of lymphopenia, hypoxemia, and bacterial coinfections, as well as with higher CT scores representing the extent of pulmonary involvement. Furthermore, multiple regression analyses indicated that possible risk factors for progressing to fatal outcome in hospitalized patients with COVID-19 pneumonia may include, but were not limited to, preexisting comorbidity, bacterial coinfection, lower SpO2 value, lower lymphocyte count, and the CT score describing the lung involvement extent.

The age-related death risk probably reflects the strength or weakness of the respiratory system, and the unbalanced sex distribution might arise from differences in underlying health conditions, not from inherent biological differences. Men have a higher incidence of chronic illnesses such as cardiovascular disease than women, and individuals with preexisting comorbidities are more likely to

experience severe or critical COVID-19 disease courses. This is in line with publications investigating this novel viral pneumonia [1,25-27].

The fundamental pathophysiology of life-threatening viral pneumonia is severe ARDS, and diffuse alveolar damage is the pathologic hallmark of ARDS. According to histological examinations, bilateral diffuse alveolar damage caused by cellular fibromyxoid exudates impairs the ability of the lungs to transfer gas from the inhaled air to erythrocytes in pulmonary capillaries. This may result in progressive respiratory failure. In the present study, SpO2 values were used as the parameter to reflect respiratory function. Ichikado et al [28,29] reported that the areas of airspace-filling attenuations (GGO or consolidation) on pulmonary CT images correspond to histologic features of the exudative or early proliferative phase of diffuse alveolar damage. In the current study, the affected lung area was evaluated using a visual CT score as an indirect parameter for respiratory function. Visual CT score analysis is straightforward compared to analyses based on computer-assisted software or machine learning algorithms; thus, this manual

scoring system is feasible in routine clinical settings without excessive scans or post processing, especially in a setting of medical emergency like the COVID-19 outbreak. The excellent inter- and intraobserver variability coefficients of our CT score demonstrated its high reliability and reproducibility to assess lung involvement. Although an indirect measure, the CT score is a relatively simple and useful method to quantify the lung involvement extent.

The frequent presence of bronchial dilations associated with various CT features of COVID-19 pneumonia was a notable finding in this study. The similar incidences of bronchial dilation found in the non-survivor and survivor groups indicated that even if the dilated bronchi influenced the short-term mortality in COVID-19 patients, this effect would depend on the extent of their associated opacities. However, they might have physiological significance for long-term survival in the survivor group. Bronchial dilation with surrounding architectural distortion, reticulation, or honeycombing indicated that these phenomena most likely represented traction bronchiectases. According to previous studies, their combined CT presence is correlated with the late proliferative or fibrotic phase of such damage [28,29]. The preliminary short-term follow-up CT in our study showed the persistence or even progress of traction bronchiectases with partial absorption of the surrounding opacities. However, a long-term follow-up with CT is still required to determine whether these traction bronchiectases are permanent and irreversible in COVID-19.

Mosaic hypo attenuation on expiratory CT images has been identified as air trapping and is considered a typical CT manifestation of small airway obstruction, although mosaic attenuation on standard inspiratory CT images might be the result of diverse causes, the mosaic attenuation associated with dilated bronchi may suggest that the mosaic pattern was secondary to small airway disease even on inspiratory CT images [30]. In the current study, CT images of 42 cases showed this combination suggesting the involvement of small airways in SARS-CoV-2 infection. However, the physiological significance of air trapping in patients recovering from SARS-CoV-2 pneumonia still require long-term follow-ups to clarify.

This retrospective cohort study had several limitations. First, some potential participants without sequential CT scans and patients still in hospitals as of March 8, 2020, were excluded; thus, the case fatality ratio in our study cannot reflect the true mortality of COVID-19. Second, the patient numbers in the non-survivor and survivor groups are unbalanced partly due to the defined exclusion criteria; thus, the results derived from our imaging and clinical findings may be biased. Third, some patients were transferred to the two study hospitals, and late-stage illnesses may have contributed to poor clinical outcomes. However, the study results still provide important information not reported before.

In conclusion, the CT involvement score is a potential predictor of the short-term outcome in patients with COVID-19. A thorough

assessment combining CT evaluation with demographic and clinical information may help establish risk stratifications and optimize treatment decisions at an early stage.

6. Declarations

Ethics approval and consent to participate: The study protocol was approved by the Ethics of Committees of The First Affiliated Hospital of China Medical University and the Union Hospital, Tongji Medical College, Huazhong University of Science and Technology, the approval number is 2020191. The requirement for informed consent was waived because the study was based on a retrospective review of medical records.

7. Funding

The National Natural Science Foundation of China (Grant No.81801661)

8. Acknowledgment

The authors would like to express their deepest appreciation to all nurses and doctors in the medical assistance team from The First Affiliated Hospital of China Medical University, as well as the staff in the Wuhan Union Hospital, Tongji Medical College, Huazhong University of Science and Technology, for their efforts against the epidemic.

References

1. Huang C, Wang Y, Li X, Ren L, Hu Y, Yin W, et al. Clinical features of patients infected with 2019 novel coronavirus in Wuhan, China. *Lancet*. 2020; 395(10223): 497-506.
2. Chen N, Zhou M, Dong X, Qu J, Yu T, Liu Y, et al. Epidemiological and clinical characteristics of 99 cases of 2019 novel coronavirus pneumonia in Wuhan, China: a descriptive study. *Lancet*. 2020; 395(10223): 507-513.
3. Zhu N, Zhang D, Wang W, Lu R, Xu W, Tan W, et al. A novel coronavirus from patients with pneumonia in China, 2019. *N Engl J Med*. 2020; 382(8): 727-733.
4. Holshue ML, DeBolt C, Lindquist S, Lofy KH, Fox L, Cohn A, et al. First case of 2019 novel coronavirus in the United States. *N Engl J Med*. 2020; 382(10): 929-936.
5. World Health Organization. Coronavirus disease (COVID-19) outbreak situation Retrieved from <https://www.who.int>. Accessed May 24, 2020.
6. China National Health Commission website. [Notice on issuing a new coronavirus infected pneumonia diagnosis and treatment plan (trial version 5)] (in Chinese). bgs.satcm.gov.cn/zhengcewenjian/2020-02-06/12847.html. Published February 4, 2020. Accessed February 18, 2020.
7. Ai T, Yang Z, Hou H, Zhan C, Sun Z, Lv W, et al. Correlation of chest CT and RT-PCR testing in coronavirus disease 2019 (COVID-19) in China: A report of 1014 cases. *Radiology*. 2020; 296(2): E32-E40.
8. Fang Y, Zhang H, Xie J, Lin M, Ji M, Pang P, et al. Sensitivity of chest CT for COVID-19: Comparison to RT-PCR. *Radiology*. 2020;

- 296(2): E115-117.
9. Bai HX, Hsieh B, Xiong Z, Liao WH, Pan I, Li S, et al. Performance of radiologists in differentiating COVID-19 from viral pneumonia on chest CT. *Radiology*. 2020; 296(2): E46-E54.
 10. Wong KT, Antonio GE, Hui DS, Lee N, Wu A, Chung SSC, et al. Thin-section CT of severe acute respiratory syndrome: evaluation of 73 patients exposed to or with the disease. *Radiology*. 2003; 228(2): 395-400.
 11. Gao F, Li M, Ge X, Lv F, Ren Q, Chen Y, et al. Multi-detector spiral CT study of the relationships between pulmonary ground-glass nodules and blood vessels. *Eur Radiol*. 2013; 23(12): 3271-7.
 12. Chan JF, Yuan S, Kok KH, To KKW, Chu H, Yang J, et al. A familial cluster of pneumonia associated with the 2019 novel coronavirus indicating person-to-person transmission: a study of a family cluster. *Lancet*. 2020; 395(10223): 514-523.
 13. Yang X, Yu Y, Xu J, Shu H, Xia J, Yu T, et al. Clinical course and outcomes of critically ill patients with SARS-CoV-2 pneumonia in Wuhan, China: a single-centered, retrospective, observational study. *Lancet Respir Med*. 2020; 8(5): 475-481.
 14. Xu Z, Shi L, Wang Y, Tai Y, Bai C, Zhu L, et al. Pathological findings of COVID-19 associated with acute respiratory distress syndrome. *Lancet Respir Med*. 2020; 8(4): 420-22.
 15. Ichikado K, Suga M, Müller NL, Ando M, Akira M, Mihara N, et al. Acute interstitial pneumonia: comparison of high-resolution computed tomography findings between survivors and nonsurvivors. *Am J Respir Crit Care Med*. 2002; 165(11): 1551-6.
 16. Ichikado K, Suga M, Muranaka H, Hirata N, Sasaki Y, Johkoh T, et al. Prediction of prognosis for acute respiratory distress syndrome with thin-section CT: validation in 44 cases. *Radiology*. 2006; 238(1): 321-9.
 17. Ichikado K, Muranaka H, Gushima Y, Suga M, Sakuma T, Nagano J, et al. Fibroproliferative changes on high-resolution CT in the acute respiratory distress syndrome predict mortality and ventilator dependency: a prospective observational cohort study. *BMJ Open*. 2012; 2(2).
 18. Nishiyama A, Kawata N, Yokota H, Uno T, Oda S, Tatsumi K, et al. A predictive factor for patients with acute respiratory distress syndrome: CT lung volumetry of the well-aerated region as an automated method. *Eur J Radiol*. 2020; 122: 108748.
 19. Guo L, Wei D, Zhang X, Wu Y, Li Q, Qu J, et al. Clinical features predicting mortality risk in patients with viral pneumonia: the MuLBSTA score. *Front Microbiol*. 2019; 10: 2752.
 20. Hansell DM, Bankier AA, MacMahon H, McLoud TC, Müller NL, Remy J. Fleischner Society: glossary of terms for thoracic imaging. *Radiology* 2008; 246(2): 697-722.
 21. Bernheim A, Mei X, Huang M, Yang Y, Lin B, Li S, et al. Chest CT findings in coronavirus disease-19 (COVID-19): Relationship to duration of infection. *Radiology*. 2020; 295(3).
 22. Pan F, Ye T, Sun P, Gui S, Li L, Wang J, et al. Time course of lung changes on chest CT during recovery from 2019 novel coronavirus (COVID-19) pneumonia. *Radiology*. 2020; 295(3): 715-721.
 23. Chung M, Bernheim A, Mei X, Yang Y, Li K, Li S, et al. CT imaging features of 2019 novel coronavirus (2019-nCoV). *Radiology*. 2020; 295(1): 202-207.
 24. Wu X, Dong D, Ma D. Thin-section computed tomography manifestations during convalescence and long-term follow-up of patients with severe acute respiratory syndrome (SARS). *Med Sci Monit*. 2016; 22: 2793-9.
 25. Zhou F, Yu T, Du R, Fan G, Liu Y, Liu Z, et al. Clinical course and risk factors for mortality of adult inpatients with COVID-19 in Wuhan, China: a retrospective cohort study. *Lancet*. 2020; 395(10229): 1054-1062.
 26. Wang D, Hu B, Hu C, Zhu F, Li Y, Cheng Z, et al. Clinical characteristics of 138 hospitalized patients with 2019 novel coronavirus-infected pneumonia in Wuhan, China. *JAMA*. 2020; 323(11): 1061-9.
 27. Guan WJ, Liang WH, Zhao Y, Li JF, Li CC, He ZX, et al. Comorbidity and its impact on 1,590 patients with COVID-19 in China: A nationwide analysis. *Eur Respir J*. 2020; 55(5): 2000547.
 28. Ichikado K, Johkoh T, Ikezoe J, Kohno N, Itoh H, Ando M, et al. Acute interstitial pneumonia: high-resolution CT findings correlated with pathology. *AJR Am J Roentgenol*. 1997; 168(2): 333-8.
 29. Ichikado K, Suga M, Gushima Y, Ando M, Itoh H, Honda O, et al. Hyperoxia-induced diffuse alveolar damage in pigs: correlation between thin-section CT and histopathologic findings. *Radiology*. 2000; 216(2): 531-8.
 30. Kligerman SJ, Henry T, Lin CT, Franks TJ, Galvin JR. Mosaic attenuation: Etiology, methods of differentiation, and pitfalls. *Radiographics* 2015; 35(5).